

Research Paper

Evaluation of GMAW Welded Joints in A36 Low-Alloy Marine Steel Sheets: Tensile Test, Hardness, and Fatigue Properties

Mohammad Reza Maraki^{1*}, Masoud Mahmoodi², Milad khodaei³, Hadi Tagimalek²

1. Department of Materials and Metallurgy Engineering, Birjand University of Technology, Birjand, Iran.

2. Faculty of Mechanical Engineering, Semnan University, Semnan, Iran.

3. Chemical Engineering Faculty, Sahand University of Technology, Tabriz, Iran.

ARTICLE INFO

Article history:

Received 30 February 2022

Accepted 18 April 2022

Available online 1 September 2022

Keywords:

Marine structures

A36 low alloy steel

Gas metal arc welding

Fatigue properties

Tensile test

Hardness

ABSTRACT

In Gas Metal Arc Welding (GMAW), the applied thermal cycle will cause a change in the chemical composition and structure of the welded zone compared to the base metal (BM). As a result, it causes changes in mechanical properties including fatigue strength. This research investigates the tensile test, hardness, and fatigue properties of A36 low-alloy marine steel with high tensile strength. For this purpose, A36 low-alloy marine steel was welded by the GMAW method. After performing the mechanical tests, the structural examination was done by optical microscope (OM) and Atomic Force Microscope (AFM) on the welded samples. The obtained results show that the fatigue strength of the weld has decreased compared to the base metal by creating coarse and heterogeneous grain structures, which are caused by the effects of the mentioned items in the weld metal. Microstructural defects in the weld metal caused cracks germination and accelerated crack growth. So that the fatigue strength of the weld metal was lower than that of the BM.

Citation: Maraki, M.R.; Mahmoodi, M.; khodaei, M.; Tagimalek, H. (2022). Evaluation of GMAW Welded Joints in A36 Low-Alloy Marine Steel Sheets: Tensile Test, Hardness, and Fatigue Properties, Journal of Advanced Materials and Processing, 10 (4), 37-44. Dor: 20.1001.1.2322388.2022.10.4.4.3

Copyrights:

Copyright for this article is retained by the author (s), with publication rights granted to Journal of Advanced Materials and Processing. This is an open – access article distributed under the terms of the Creative Commons Attribution License (<http://creativecommons.org/licenses/by/4.0>), which permits unrestricted use, distribution and reproduction in any medium, provided the original work is properly cited.



*** Corresponding Author:**

E-Mail: maraki@birjandut.ac.ir

1. Introduction

Fatigue is one of the main failure factors in welded structures, which occurs due to the application of alternating forces lower than the ultimate strength (UTS) and often lower than the yield point [1]. Fatigue criteria should be considered when designing and producing welded structures. In the design step, the geometry and loading force of Gas Metal Arc Welding (GMAW) welded samples is one of the essential parameters [2]. GMAW welding defects are unavoidable in welded structures and these defects have significant effects on the strength of welded marine structures [3,4]. Fatigue life prediction of welded joints is expensive, time-consuming, and requires repeated testing. These complications are caused by the weld complex geometry, stress concentration, and heterogeneity of weld metal properties [5,6]. Therefore, to avoid the complicated and expensive method, traditionally, weld joints life used in marine structures is performed by the stress-life curve (S-N) [7,8]. To increase the strength in marine structures, A36 steels are usually used with higher tensile strength and fatigue resistance than plain carbon steel. A36 steel is a kind of low-carbon steel. Low-carbon steels with less than 0.3% carbon by weight are classified in this category. This allows A36 steel to be easily machined, welded, shaped, and used as general-purpose steel [9]. Low carbon also avoids the effect of heat treatment on A36 steel. A36 steel usually also contains small amounts of other alloying elements, including manganese, sulfur, phosphorus, and silicon [10]. These alloying elements are added to create specific chemical and mechanical properties. Since A36 steel does not contain much nickel or chromium, its corrosion resistance is not high. This problem is one of the prominent features of A36 steel chemical compounds. GMAW welding is a complex process that, by applying thermal stresses, solid phase transformation, leads to metallurgical changes, and this causes a local increase in stress [11]. Due to non-uniform temperature gradient and thermal expansion and contraction, which causes local plastic deformation during the GMAW welding process. In addition to these residual stresses, different and unavoidable discontinuities in GMAW welding create places for the germination and growth of fatigue cracks. Fatigue cracks in such places easily germinated and grow, which reduces the lifetime of the sample [12]. In the GMAW welding process, mechanical and metallurgical defects and structural

changes can be suitable places for the germination and growth of fatigue cracks [13]. Fatigue cracks usually germinate and grow from the surface or the place of internal defects [14].

Marine structures are affected by hydrodynamic forces caused by water turbulence, hence the issue of fatigue in these structures is raised and the phenomenon of fatigue and its investigation in ships and marine structures is of particular importance. In this research, the fatigue properties in the GMAW process on the marine structures on A36 low-alloy sheets (used in the petrochemical industry) have been investigated. In this research, for the first time, the fatigue properties of marine structures on A36 low-alloy sheets connected by GMAW welding operation have been discussed.

2. Experimental method

MIG welding is a type of welding, also known as GMAW. In this type of welding, the electric arc creates a heat source that is created by the consumable electrode. The consumable electrode used in this process is made of metal, and the arc created between them causes the part to heat up. The gas used in this type of process is an inert gas, such as helium or argon. In this research, A36 low-alloy steel sheets with high tensile strength, widely used steels in the marine industry, were used. GMAW welding (Figure 1) electrode used is to AWS/ASMS SFA-5.28 (ER 80S-G ER80S-Ni1) type with high tensile strength. The thickness of the sheets is 10 mm and the diameter of the used electrode is 2 mm, which is presented in Table 1 with both chemical compositions. To determine the chemical composition, the samples were chemically analyzed using optical emission spectrometry (OES). Table 2 showed the mechanical properties of A36 steel and GMAW electrode. The AWS/ASMS SFA-5.28 (ER 80S-G ER80S-Ni1) electrode contains nickel, chromium, and copper alloys used for GMAW welding resistant to atmospheric corrosion, and due to its mechanical properties, it is suitable for welding steels with high resistance and impact. This wire can be used with CO_2 gas and other gas mixtures such as Ar gas with 5 ~ 25% CO_2 . The AWS/ASMS SFA-5.28 (ER 80S-G ER80S-Ni1) electrode was heated in an industrial furnace to a temperature of 350 °C for two hours. After GMAW welded the samples, samples electrical discharge machining by a magnetic saw. Table 3 shows the conditions and process characteristics of the current research.

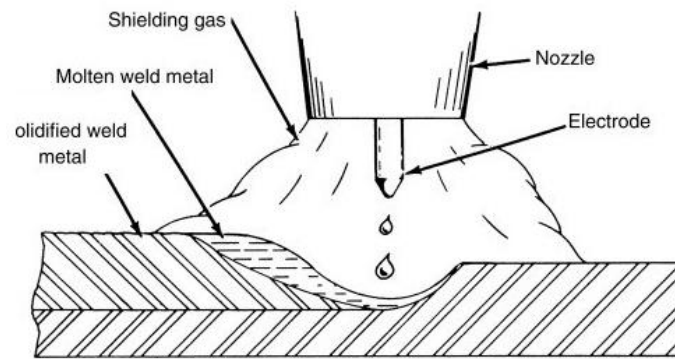


Fig. 1. GMAW schematic

Table 1. Chemical composition of A36 steel and GMAW electrode

	Fe	P	S	Ni	Mn	Si	C	Cu
A36 steel	Bal	0.04	0.05	--	0.62	0.42	0.25	0.20
AMA 80-12M	Bal	< 0.02	< 0.02	2.3	1.2	0.5	0.08	--

Table 2. Mechanical properties of A36 steel and GMAW electrode

	Compact strength	Elongation	Yield stress	Tensile strength
Unit	Joule	%	N/mm ²	N/mm ²
A36 steel	> 54	20	250	550
AMA 80-12M	> 47	> 22	> 460	550-700

Table 3. Conditions and process characteristics of the current research

Ex	Speed welding (cm/min)	Number pass	repeatability	Welding type and approval
#1	0	0	0	0
#2	7.63	3	2	Visual test (VT)
#3	8.14	6	2	Visual test (VT)
#4	8.02	9	2	Visual test (VT)

In the following, the mechanical properties including tensile test, hardness and fatigue were investigated. After performing the mechanical tests, structural examination was performed by optical microscope (OM) and atomic force microscope (AFM) on the welded samples. The ASTM E8M standard defines test methods and requirements for determining the stress-strain relationship of materials using uniform tensile tests. To check the fatigue strength of samples, yield strength and ultimate strength of samples should be measured. For this purpose, a tensile test was first performed on seven samples (#1, two #2, two #3, and two #4) as shown in Figure 2. Seven samples were subjected to a tensile test by STM 400. According to the ASTM E466 standard, to perform the fatigue test, the maximum force used for failure should be selected based on the UTS strength of the sample [15]. All fatigue tests were performed under direct axial loading on a servo-hydraulic fatigue test machine under load control and at ambient temperature (approximately 20°C). The samples were loaded by the STM 400 fatigue testing machine

in the form of tension-compression. According to the final strength of the samples, the maximum force applied to them was determined. According to the ASTM E466 standard, the fatigue cycle at R=-1 was considered as maximum and minimum [16].

3. Results and discussion

3.1. Tensile test

Tensile samples failed due to necking and stress-strain curves were obtained as shown in Figure 3. The necking area at the point of plastic instability where the increase in strength due to work hardening is reduced to compensate for the reduction in the cross-sectional area. According to the data obtained in the tensile test, based on the ultimate strength (UTS), the stresses applied to the fatigue samples were determined. By comparing the results of the tensile strength of the weld metal and the base metal, it is clear that the tensile strength of the weld metal was lower than the tensile strength of the base metal. UTS is 3 passes, A36 steel base metal, 6 passes, and 9 passes respectively.

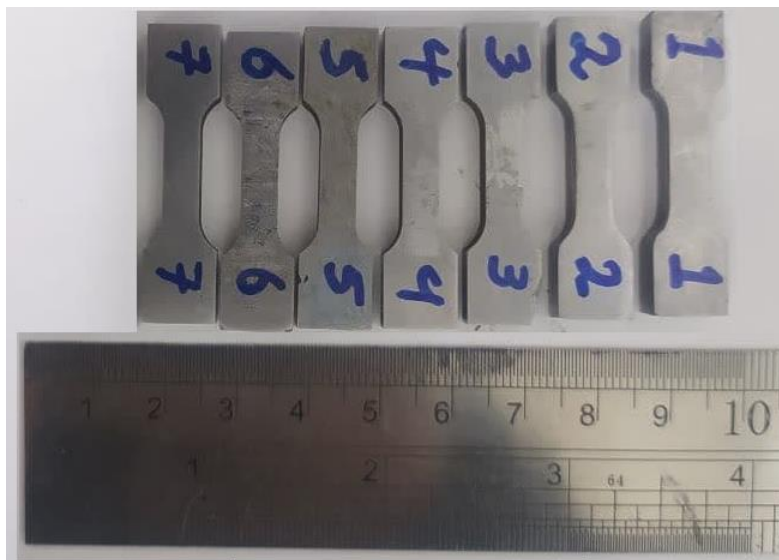


Fig. 2. Samples prepared in GMAW ed

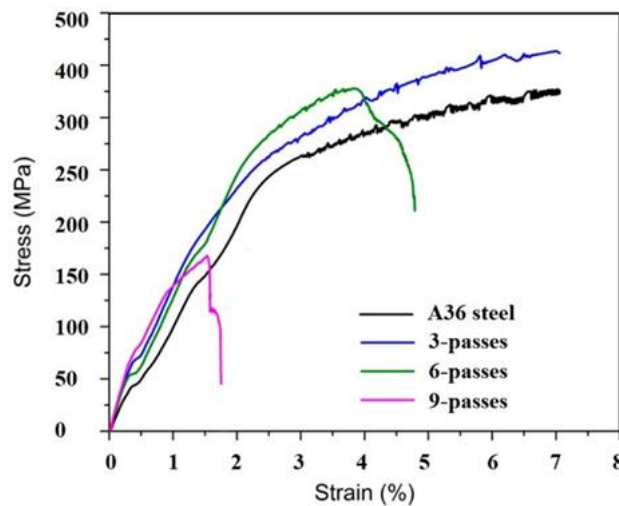


Fig. 3. Stress-strain curve

3.2. Fatigue test

Fatigue test samples were prepared from welded sheets according to ASTM E466 standard in seven samples so that the weld metal was placed in the center of the sample. A fatigue test was performed in the form of tension-compression at the frequency of 3 Hz and $R = -1$ on the samples. In the welded structures, due to the thermal cycle, the structure of the weld metal changes compared to the base metal,

and thermal contraction after GMAW welding causes the creation of heterogeneous and hard structures in the weld metal. These heterogeneous structures in the weld metal are prone to fatigue cracking compared to the base steel which has a uniform structure. Therefore, the place of failure has been often in the GMAW welding area. Therefore, all samples cracked and fractured with an inclined angle and from the weld zone (Figure 4).

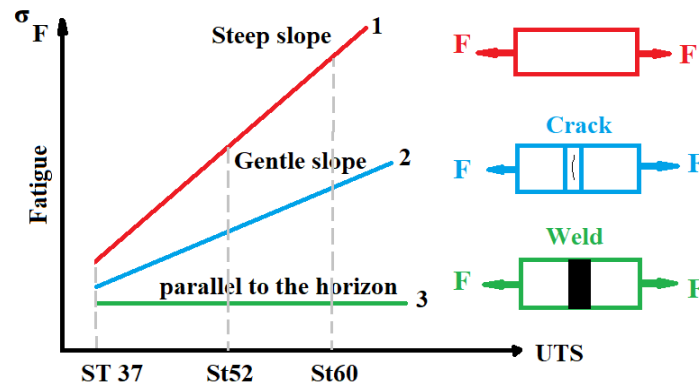


Fig. 4. Type and slope in fatigue/UTS diagram

Table 4. Result tension-compression

Samples	Cycles Number			
	#1	#2	#3	#4
Results	32244	113298	98520	100045
		117053	99362	105324
Stress (MPa)	400	400	450	500

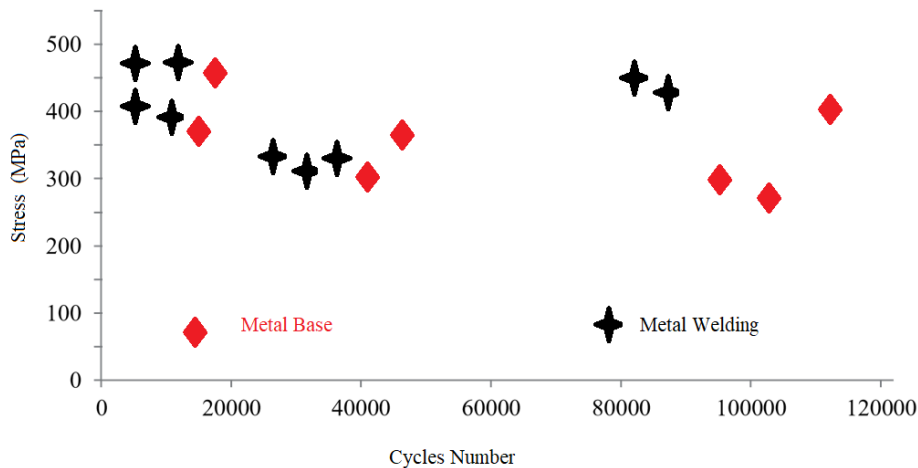


Fig. 5. Stress-cycle curve

Due to the dispersion of data in the fatigue test, two samples were tested at each stress level and the number of cycles obtained at each stress level was recorded according to Table 4. Based on these results, the stress-cycle curve was obtained according to Figure 5.

As can be seen from the fatigue diagram, as the applied stress decreases, the number of failure cycles increases, but the fatigue strength of the weld metal is lower than that of the A36 steel. The comparison of the results of the tensile test in the weld sample and the base steel was consistent with the results obtained from the fatigue test. In the welded parts, due to the subsurface defects, which are part of the intrinsic defects, less time and number of cycles are spent on crack initiation. As a result, the major part of the fatigue life in such parts is spent on crack growth and propagation until the final failure. In non-welded steels, about 90% of the fatigue time until the occurrence of the final failure is related to the fatigue

crack initiation time, and only 10% of the total time is related to the stable growth of the fatigue crack. On the contrary, due to the presence of microscopic defects in welded joints, the germination stage is practically achieved before the start of fatigue loading in GMAW welding operations, and the fatigue time is only related to the time of stable growth of fatigue cracks.

3.3. Hardness

For broken samples, hardness was measured using 25 gr and 5 seconds with a magnification of 400 in the broken site. In each sample, the average of twelve hardness measurements is calculated and presented in Figure 6. The comparison of these results shows that at the fracture surface of the base metal, the hardness is higher than that of the weld metal, which is consistent with the results obtained from the tensile test.

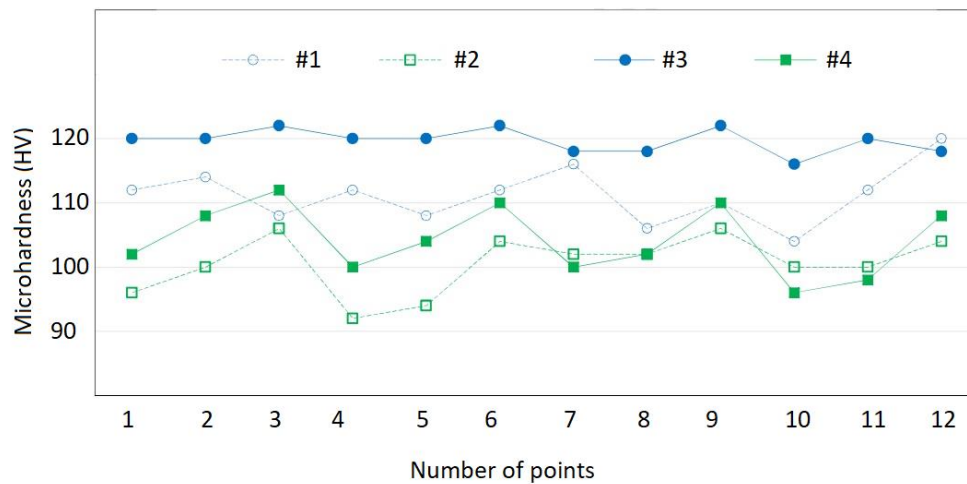


Fig. 6. Hardness results in the failure zone

Some samples were engraved in a 2% Nital solution to check metallography. In addition, AFM analysis and hardness measurement operations were also performed on the fracture site. The OLYMPUS BX51M optical microscope was used to identify the structure in the base metal, and weld metal. Figure 6 shows the optical microscopy of the base metal, #2,

#3 and #4. As can be seen, the microstructure of the base metal is composed of ferrite with uniform grains. Due to the thermal and rolling operations that are carried out in its production process, the base steel has a uniform structure with almost homogeneous grain size.

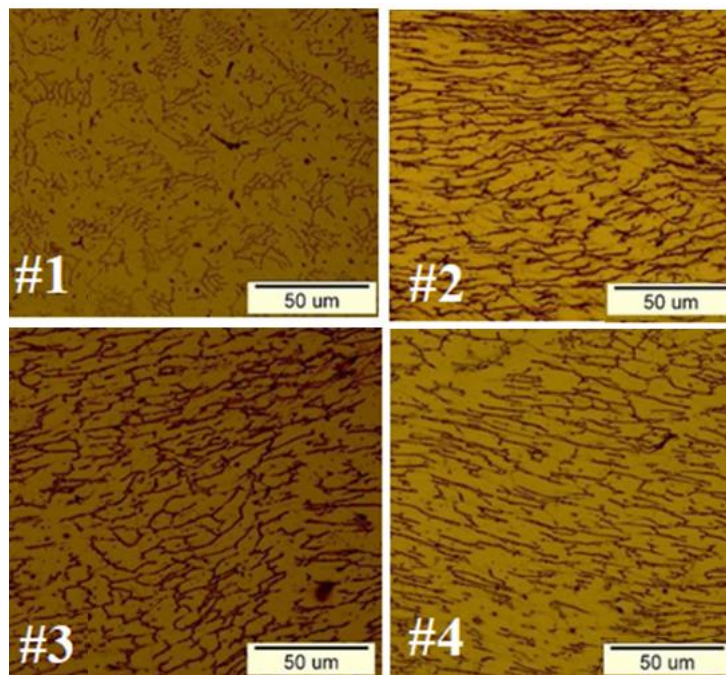


Fig. 7. Optical microscopic image of specimens #1, #2, #3 and #4 (200 magnifications)

The size of the grains in the upper layers is in the form of columnar grains due to the connection with the ambient air, but in the lower layers, due to the thermal process caused by the upper layers, they have recrystallized and as a result, the grains have become smaller.

The structural investigation showed that the structure in the weld metal was of heterogeneous coarse-grained ferrite and Widmanstätten structure, but the

structure of the base metal was homogeneous fine-grained ferrite metal (Figure 7). In welding metal, due to thermal cycles applied during GMAW welding, it had a different structure from the base metal. In general, finer grain sizes have better fatigue strength than coarse grains, except at high temperatures where there is creep/fatigue interaction. Finer grains reduce the regional strains along the slip bands and reduce the number of return slips.

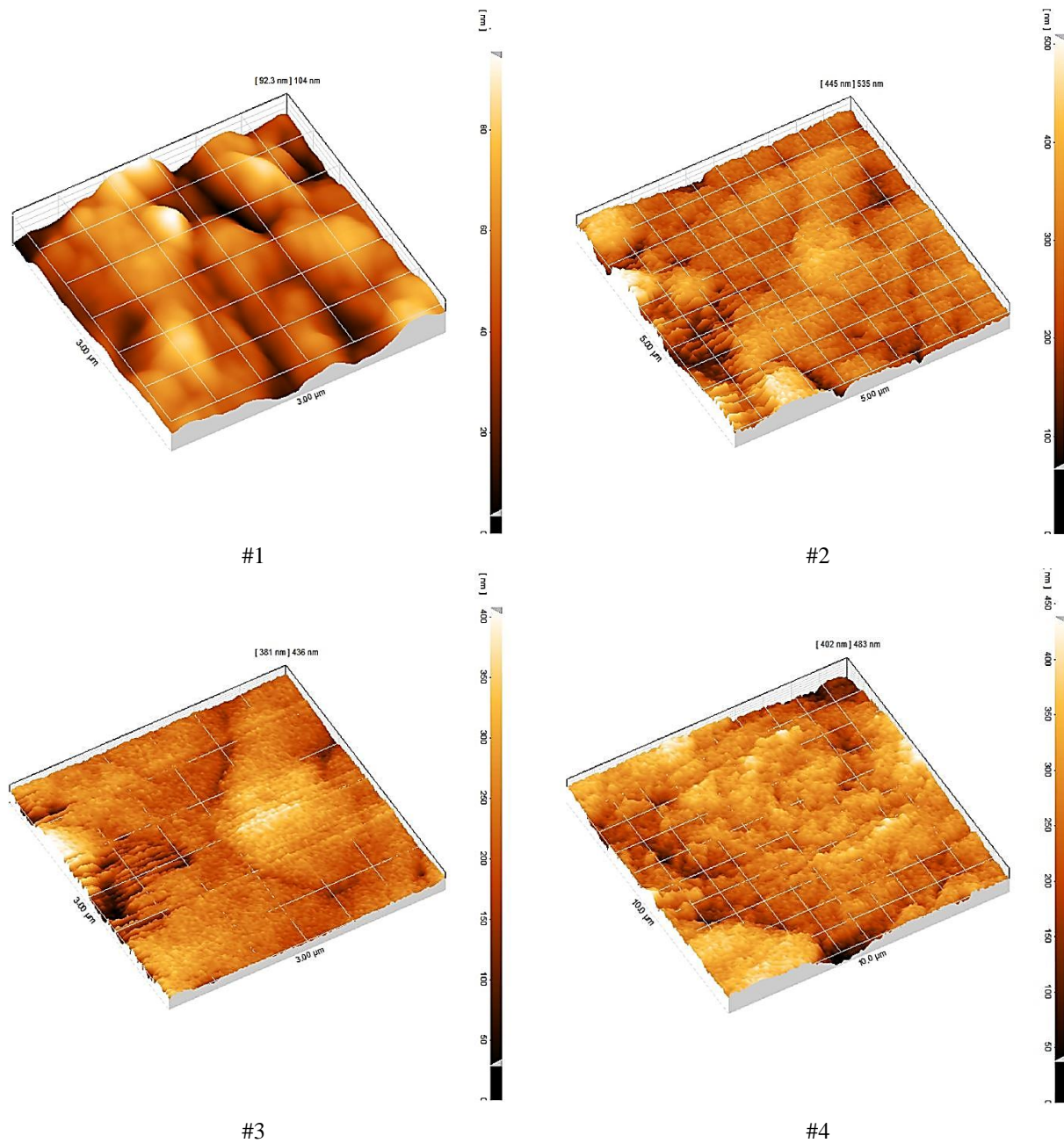


Fig. 8. AFM images of the #1, #2, #3 and #4 samples

In Figure 8, the values obtained based on the changes in grain size and the value of the error bar for a specific interval of about 100 nm are shown as standard deviation. At high strains, the dislocations start to move in the directions of the active sliding systems of the samples under the GMAW welding process. Dislocations collide with each other inside the grains and accumulate in areas next to each other, with the increase of cycles, the density of dislocations in these areas increases. The density of dislocations is formed in different parts of the sample. Examination of the topography of the fracture surface showed that it is quite evident with the changes in the effective parameters. The results of AFM showed that the surface dislocation is in the range of 400 nm

and the most suitable sample is #1, #3, #4, and #2 respectively.

4. Conclusions

In this research, the fatigue strength of weld metal and base metal in marine low alloy steel was investigated and the following results were obtained:

- Due to the reduction of fatigue strength in the weld metal region compared to the base metal, the weld metal of low-alloy steel with high tensile strength does not necessarily show better fatigue strength than the weld metal of mild steel in the same GMAW welding.
- The cycle of thermal operations applied during GMAW welding and fusion of the base metal with

the consumable electrode causes a change microstructure of the base steel from a ferritic structure to a Widmanstätten structure and coarse-grained ferrite and causes metallurgical and microstructural defects in the welding.

- The microstructural defects in the weld metal cause crack germination and crack growth to accelerate so that the fatigue strength of the weld metal is lower than that of the base metal.
- Fine-grained ferrite structures reduce regional strains along slip bands and provide more grain boundaries to help stop cracking and deformation.
- It is necessary to achieve a desirable structure with suitable mechanical properties by following proper GMAW welding instructions and controlling the input heat.
- By increasing the grain size and structural heterogeneity and on the other hand by increasing the percentage of Widmanstätten ferrite as the reference path for fatigue crack growth, the fatigue life of the welded samples decreases.
- Widmanstätten ferrite grain boundaries are on the best path for crack growth, and with the presence of Widmanstätten ferrite in the structure of the weld metal, the fatigue strength in the weld metal is reduced or worsened.

Reference

- [1] Z. Jie, K. Wang, S. Liang., "Residual stress influence on fatigue crack propagation of CFRP strengthened welded joints", *Journal of Constructional Steel Research*, Vol. 196, 2022, 107443.
- [2] S. Han, G. Liu, X. Tang, L. Xu, H. Cui, C. Shao., "Effect of molten pool behaviors on welding defects in tandem NG-GMAW based on CFD simulation", *International Journal of Heat and Mass Transfer*, Vol. 195, 2022, 123165.
- [3] P. Hariprasath, P. Sivaraj, V. Balasubramanian, Srinivas Pilli, K. Sridhar., "Effect of the welding technique on mechanical properties and metallurgical characteristics of the naval grade high strength low alloy steel joints produced by SMAW and GMAW", *CIRP Journal of Manufacturing Science and Technology*, Vol. 37, 2022, pp584-595.
- [4] H. Tagimalek, M. Azargoman, M.R. Maraki, M. Mahmoodi., "The effects of diffusion depth and heat-affected zone in NE-GMAW process on SUH 310S steel using an Image processing method", *International Journal of Iron & Steel Society of Iran*, Vol. 17, Issue. 1, 2020, pp. 11-20.
- [5] L. Su, Z. Fei, B. Davis, H. Li, H. Bornstein., "Digital image correlation study on tensile properties of high strength quenched and tempered steel weld joints prepared by K-TIG and GMAW", *Materials Science and Engineering: A*, Vol. 827, 2021, 142033.
- [6] S.C. Siriwardane, N.D Adasooriya, D. Pavlou., "Fatigue Strength Curve for Tubular Joints of Offshore Structures under Dynamic Loading" *Dynamics*, Vol. 1, 2021, pp. 125–133.
- [7] A. Mohammadipour, K. Willam., "A numerical lattice method to characterize a contact fatigue crack growth and its Paris coefficients using configurational forces and stress-life curves", *Computer Methods in Applied Mechanics and Engineering*, Vol. 340, 2018, pp. 236-252.
- [8] R. Yu, X. Li, Z. Yue, A. Li, Z. Zhao, X. Wang, H. Zhou, T.J. Lu., "Stress state sensitivity for plastic flow and ductile fracture of L907A low-alloy marine steel: From tension to shear", *Materials Science and Engineering: A*, Vol. 835, 2022, 142689.
- [9] Z.Chen, L. Sun, W. Zhang, H. Zheng, W. Xia, H. Zeng, S. Chen, K. Li, W. Li., "Corrosion behavior of marine structural steel in tidal zone based on wire beam electrode technology and partitioned cellular automata model", *Corrosion Communications*, Vol. 5, 2022, pp. 87-97.
- [10] N. Zhao, Q. Zhao, Y. He, R. Liu, W. Liu, W. Zheng, L. Li., "Strengthening-toughening mechanism of cost-saving marine steel plate with 1000 MPa yield strength", *Materials Science and Engineering: A*, Vol. 831, 2022, 142280.
- [11] C. Ren, H. Wang, Y. Huang, Q.Q. Yu., "Post-fire mechanical properties of corroded grade D36 marine steel", *Construction and Building Materials*, Vol. 263, 2020, 120120.
- [12] J. Ge, Y. Sun, S. Zhou., "Fatigue life estimation under multiaxial random loading by means of the equivalent Lemaitre stress and multiaxial S–N curve methods", *International Journal of Fatigue*, Vol. 79, 2015, pp. 65-74.
- [13] P.D.T. Caiza, S. Sire, T. Ummerhofer, Y. Uematsu., "Full and partial compression fatigue tests on welded specimens of steel St 52-3. Effects of the stress ratio on the probabilistic fatigue life estimation", *Applications in Engineering Science*, Vol. 10, 2022, 100091.
- [14] Q. Gao, H. Xin, J.A.F.O. Correia, A.S. Mosallam, F. Berto., "Probabilistic fatigue life analysis considering mean stress effects of fiber reinforced polymer (FRP) composites", *International Journal of Fatigue*, Vol. 162, 2022, 106951.
- [15] J. Brnic, S. Balos, M. Brcic, M. Dramicanin, S. Krscanski, M. Milutinovic, B. Ding, Z. Geo., "Testing and analysis of uniaxial mechanical fatigue, charpy impact fracture energy and microhardness of two low-carbon steels", *Materials*, Vol. 16, 2023, 884.
- [16] H. Zhao, J. Liu, F. Hua, Y. Ran, R. Zi, B. Li., "Multiaxial fatigue life prediction model considering stress gradient and size effect", *International Journal of Pressure Vessels and Piping*, Vol. 199, 2022, 104703.